A Three-Arm Scaffold Carrying Affinity Molecules for Multiplex Recognition Imaging by Atomic Force Microscopy: The Synthesis, Attachment to Silicon Tips, and Detection of Proteins

ARTICLE *in* JOURNAL OF THE AMERICAN CHEMICAL SOCIETY · MAY 2015

Impact Factor: 12.11 · DOI: 10.1021/jacs.5b03079 · Source: PubMed

JACS
JOURNAL OF THE AMERICAN CHEMICAL SOCIETY

Article

pubs.acs.org/JACS

A Three-Arm Scaffold Carrying Affinity Molecules for Multiplex Recognition Imaging by Atomic Force Microscopy: The Synthesis, Attachment to Silicon Tips, and Detection of Proteins

Saikat Manna,[†,‡] Subhadip Senapati,[†,‡] Stuart Lindsay,*[,†,‡,§] and Peiming Zhang*[,†]

[†]Biodesign Institute, [‡]Department of Chemistry and Biochemistry, and [§]Department of Physics, Arizona State University, Tempe, Arizona 85287, United States

Supporting Information

ABSTRACT: We have developed a multiplex imaging method for detection of proteins using atomic force microscopy (AFM), which we call multiplex recognition imaging (mRI). AFM has been harnessed to identify protein using a tip functionalized with an affinity molecule at a single molecule level. However, many events in biochemistry require identification of colocated factors simultaneously, and this is not possible with only one type of affinity molecule on an AFM tip. To enable AFM detection of multiple analytes, we designed a recognition head made from conjugating two different affinity molecules to a three-arm linker. When it is attached to an AFM tip, the recognition head would allow the affinity molecules to function in concert. In the present study, we synthesized two recognition heads: one was composed of two nucleic acid aptamers, and the other one composed of an aptamer and a cyclic peptide. They were attached to AFM tips through a catalyst-free click reaction. Our imaging results show that each affinity unit in the recognition head can recognize its respective cognate in an AFM scanning process independently and specifically. The AFM method was sensitive, only requiring 2 to 3 μL of protein solution with a concentration of ~2 ng/mL for the detection with our current setup. When a mixed sample was deposited on a surface, the ratio of proteins could be determined by counting numbers of the analytes. Thus, this mRI approach has the potential to be used as a label-free system for detection of low-abundance protein biomarkers.

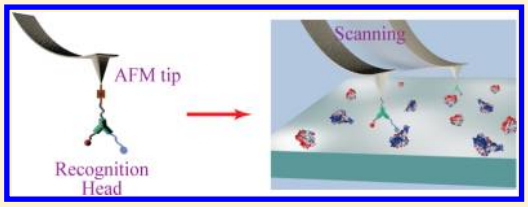

INTRODUCTION

Atomic force microscopy (AFM), a surface imaging tool with nanometer spatial resolution, has been evolved into a molecular nanobiotechnique,[1] used in imaging of proteins on solid surfaces and on living cells,[2,3] supramolecular assembly,[4] and hydrogen bonding complexes,[5,6] as well as in measurement of interacting forces between proteins,[7−9] protein and DNA,[10] and between ligand and receptor[11−13] at a single molecule level in physiological environments. With high speed AFM,[14] as an example, antibodies walking on bacterial surfaces can be monitored on a time scale of 0.01−1 s/step.[15] AFM provides a unique means of detecting proteins with potential applications in proteomics[16] and diagnostics of cancer.[17] Furthermore, the capabilities of AFM to sense chemical entities continue to improve with better methods of tip functionalization. For example, when an antibody attached to an AFM tip through a polyethylene glycol (PEG) linker is brought to scan a surface, it will generate a map of the location of its antigen molecules because of the specific intermolecular interactions, a technique known as Recognition Imaging,[18] which has been extended to epigenomics for determination of DNA methylation patterns.[19] Thus, one can conceive of using the recognition imaging for detection of low-abundance proteins in a biological sample. Compared to fluorescence microscopy, however, the AFM based recognition imaging lacks a multiplex capacity to detect multiple analytes in a single test. Wang et al. attempted to address the multiplexing issue by functionalizing AFM tips with an equimolar mixture of two types of antibodies.[20] This approach attaches the antibody molecules to the apex of an AFM tip completely by random chance. As a result, it only showed marginal success in the multiplex recognition imaging. The challenge has been how to tether two different affinity molecules to the AFM tip so that they can interact with their respective cognates with an equal probability. In the present study, we have developed a "recognition head" built on a three-arm linker that can carry affinity molecules and be connected to AFM tips for the multiplex recognition imaging (mRI). As illustrated in Figure 1, when such a recognition head tethered to an AFM tip scans across a surface covered with proteins, the two affinity moieties are bought to contact with each of these individual molecules, which generates a recognition image to localize each of cognate proteins through the specific affinity interactions. To identify each of these proteins, one of the affinity moieties in the recognition head will be blocked, for example, with its cognate protein for a second scan over the same area. This would allow us to distinguish between two different proteins. Here, we report on synthesis of the recognition heads, their attachment to AFM tips, and implementation in detecting proteins.

Received: March 24, 2015
Published: May 21, 2015

DOI: 10.1021/jacs.5b03079
J. Am. Chem. Soc. 2015, 137, 7415−7423

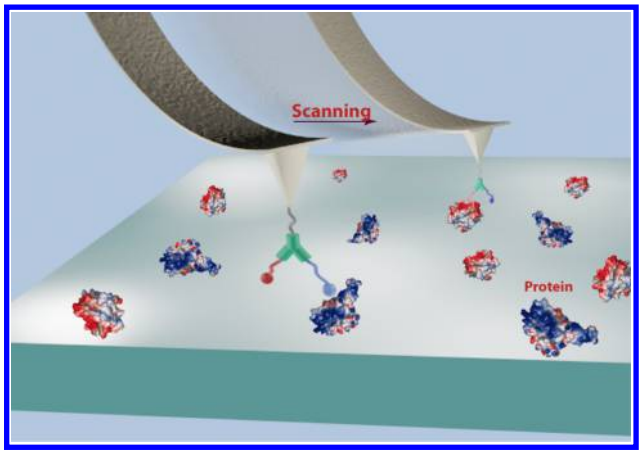

Figure 1. Illustration of multiplex recognition imaging with an AFM tip functionalized with a recognition-head containing two affinity molecules through a three-arm linker.

RESULTS AND DISCUSSION

Three-Arm Linker. We devised a C_3-symmetrical linking molecule with functional groups at its ends (**Ar3**, Scheme 1) as a scaffold for construction of the recognition heads. Although heterotrifunctional linkers are advantageous for orthogonal bioconjugation,[21,22] a homotrifunctional linker has the advantages of simpler synthesis and reduced structural variations at the linkage sites. We synthesized **Ar3** by reacting 1,3,5-triethynylbenzene (**1**) with 1-azido-37-(4-iodophenyl)-$3n_{36}^3$-dodecaoxaheptatriacontane (**2**, see Section 1 in Supporting Information for its synthesis) under the Sonogashira coupling conditions (Reaction 1.1).[23] The product was obtained with a 35% yield, purified with column chromatography, and fully characterized with NMR, and mass spectrometry (see Experimental Section).

The three-arm linker **Ar3** features a rigid hard core flanked by three flexible poly(ethylene glycol) (PEG) chains with azido functions at their ends for the bioconjugation and attachment. In general, the recognition imaging requires a fairly long linker to tether the affinity molecule to an AFM tip so that it can keep the AFM tip away from a substrate for most of the measurement period. A PEG chain with 12−18 units of ethylene glycol meets this requirement and suffices to accurately locate the binding sites of analyte molecules immobilized on a surface.[24,25] This is why it is commonly used as a flexible linker for the recognition imaging. By contrast, we designed the three-arm linker differently by placing a sizable hard core in the center of the linker, attempting to reduce the flexible portion of the linker to a minimum without affecting the binding efficiency of the affinity moieties. Thus, the increased rigidity should reduce the loss in conformational and rotational entropy caused by binding to the target molecule(s) immobilized on the surface, which is thermodynamically unfavorable.[26] We adapted tris(phenylethynyl)benzene due to its large π conjugating structure to increase the rigidity of the linker as well as to avoid the possible collision between two affinity moieties by pointing them in opposite directions. Meanwhile, we have to ensure that the linker has sufficient solubility for the following bioconjugating reactions. We found that three 12-unit PEG chains were needed to give the linker the solubility of ~0.1 mg/μL in aqueous solution when they were attached to the 4′ position of tris(phenylethynyl)benzene hard core (see Scheme 1).

Conjugating Affinity Molecules to the Three-Arm Linker. We have constructed two recognition heads: **RH-1**, which is composed of anti-VEGF[27] and anti-TNFα[28] DNA aptamers (Figure 2A), and **RH-2**, which is composed of anti-thrombin aptamer[29,30] and cyclo-RGDfK that binds to integrin receptors[31] (Figure 2B), for the mRI studies. These aptamers have nanomolar affinities to their respective cognate proteins (K_d: 403.6 nM for anti-VEGF,[27] 7.0 nM for anti-TNFα,[28] 240 ± 16 for anti-thrombin[32]), and the cyclo-RGDfK binds to both intergrin $\alpha_5\beta_1$ and $\alpha_v\beta_3$ with IC_{50} of 133 and 2.6 nM.[33] Previously, we demonstrated that both cyclo-RGDfK and anti-thrombin aptamer could effectively generate recognition images with their cognate proteins when they were attached to AFM tips through a linear linker.[34] Compared to antibodies, these affinity molecules are much smaller in size and chemically more robust, making them ideal candidates for construction of the recognition heads. To attach them to the three-arm linker, each of these custom-synthesized DNA aptamers was synthesized to

Scheme 1. Reaction for Synthesis of the Three-Arm Linker

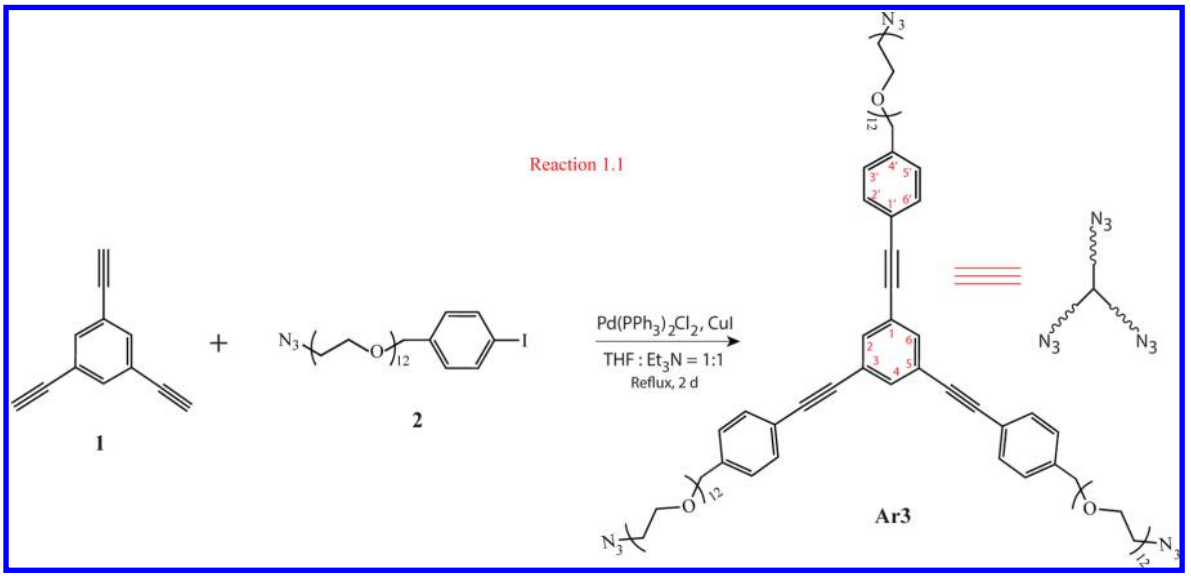

DOI: 10.1021/jacs.5b03079
J. Am. Chem. Soc. 2015, 137, 7415−7423

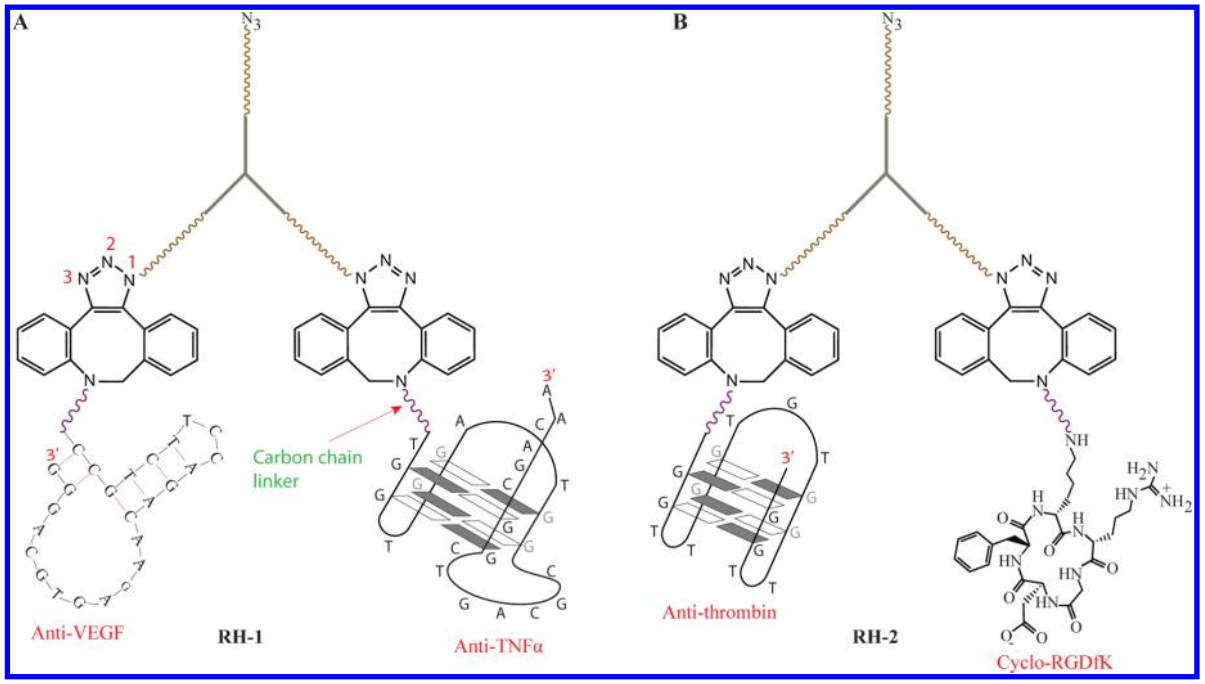

Figure 2. Illustration of chemical structures of recognition heads: (A) **RH-1** that is composed of anti-VEGF and anti-TNFα; (B) **RH-2** that is composed of anti-thrombin and cyclo-RGD. Anti-VEGF and anti-TNFα aptamers were drawn according to secondary structures proposed in literature (refs 29 and 30), and anti-thrombin aptamer according to its structure in solution (ref 31).

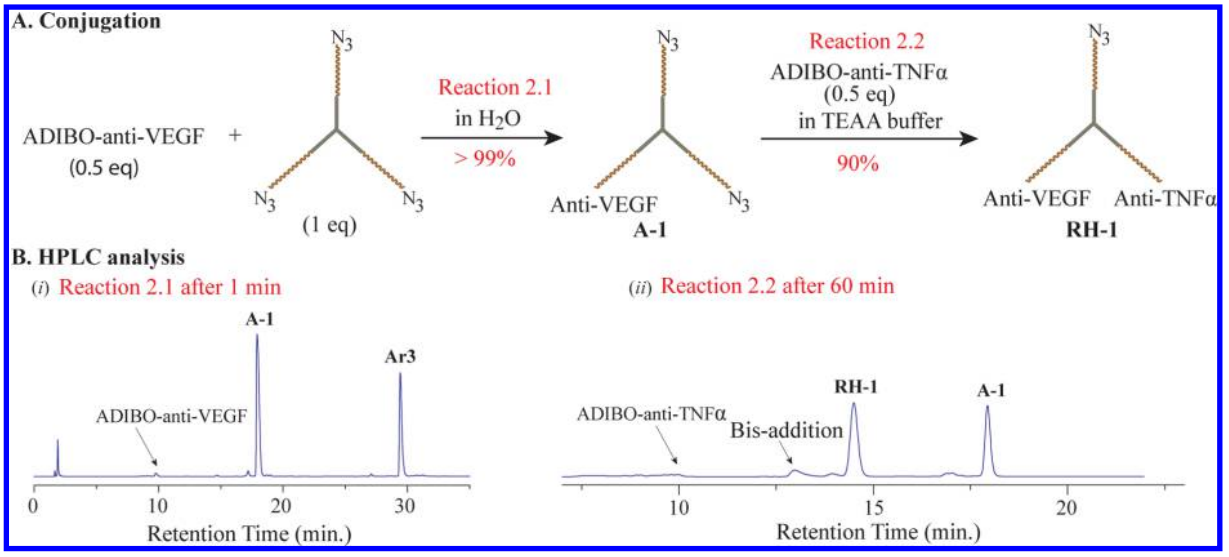

Figure 3. (A) Synthetic route to **RH-1**; (B) RP HPLC chromatograms of reaction mixtures, recorded by a UV detector at 254 nm.

bear a dodecylamino chain at their 5′-ends and the cyclopeptide contained a lysine residue. We converted them into aza-dibenzocyclooctyne (ADIBO) derivatives, named as ADIBO-anti-VEGF, ADIBO-anti-TNFα, ADIBO-anti-Thrombin, and ADIBO-cyclo-RGD, by reacting with ADIBO-*N*-hydroxysuccinimidyl ester (see Sections 2 and 3 in Supporting Information for their synthesis and characterization in detail). The ADIBO group spontaneously reacts with azide in aqueous solution, known as catalyst-free click addition,[35,36] which has allowed us to readily construct the recognition heads, as discussed below.

We synthesized **RH-1** with a route described in Figure 3A. First, ADIBO-anti-VEGF reacted with **Ar3** with a ratio of 1:2 in water (Reaction 2.1 in Figure 3). Reverse Phase (RP) HPLC analysis indicated that the reaction was finished in less than 1 min, forming a monoaddition product **A-1** with a high yield (>99%, Figure 3B,*i*). We attribute the high selectivity to the solvent condition. In water, the negatively charges of an aptamer is much less shielded than in the buffered solution. Once one aptamer was attached to **Ar3**, the second addition of an aptamer stalled because of the electrostatic repulsion. **A-1** was separated by HPLC and characterized as a pure product (see details in **RH-1** of Experimental Section). It reacted with ADIBO-anti-TNFα (0.5 equiv) in a triethylammonium acetate (TEAA) buffer (Reaction 2.2), resulting in the desired product **RH-1** with a yield of ~90% plus ~10% of a bis(anti-TNFα) byproduct (Figure 3B, *ii*). Beforehand, we had attempted to carry out the reaction in water, and found out that it went so slowly that no significant amount of product was observed even after 1 h. We hypothesized that the charge repulsion prevented

DOI: 10.1021/jacs.5b03079
J. Am. Chem. Soc. 2015, 137, 7415−7423

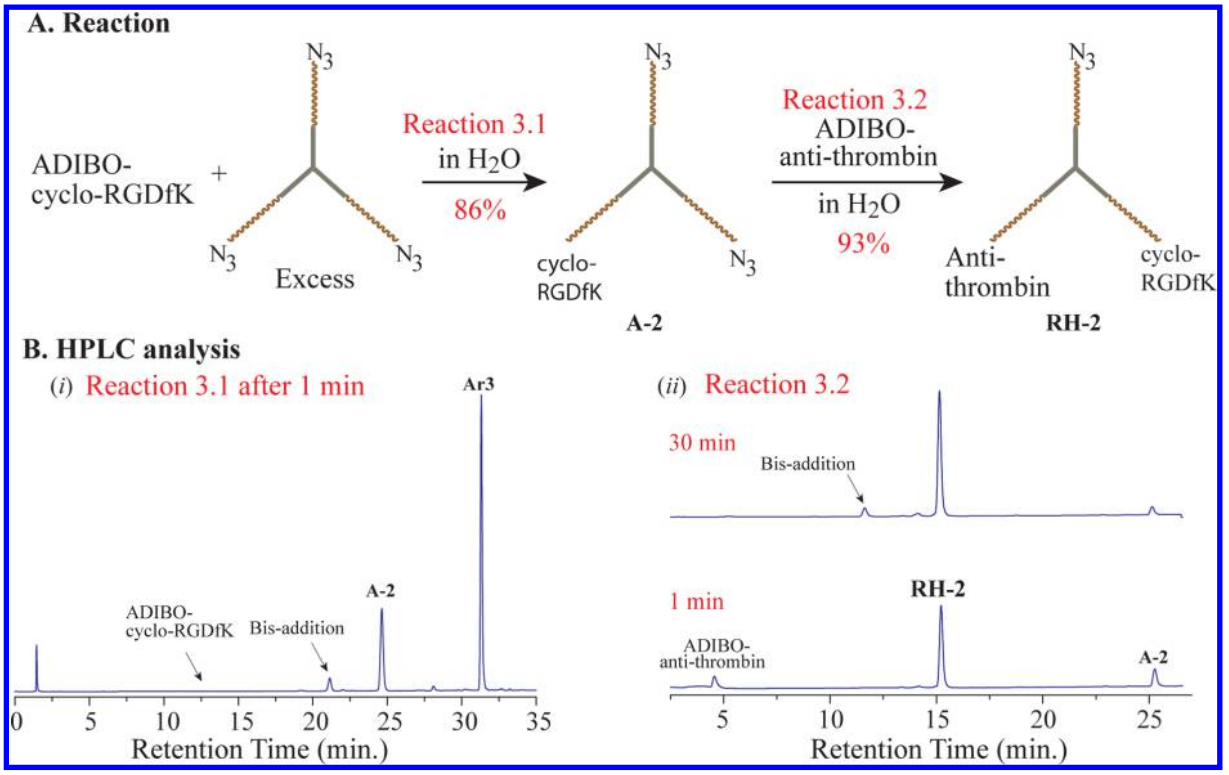

Figure 4. (A) Synthetic route to **RH-2**; (B) RP HPLC chromatograms of reaction mixtures with time, recorded by a UV detector at 280 nm for Reaction 3.1 and 254 nm for Reaction 3.2.

A-1 from reacting with the same negatively charged reactant ADIBO-anti-TNFα. A TEAA buffer was used for the reaction to shield the negative charges, giving us a fairly good selectivity (~90%) as mentioned above. **RH-1** were separated by HPLC and characterized by MALDI mass spectrometer (see **RH-1** in Experimental Section).

RH-2 was synthesized by first reacting with peptide (ADIBO-cyclo-RGD) and then with aptamer ADIBO-anti-thrombin (Figure 4A). This route offered advantages over the other way around with better control over the addition of the affinity molecules to **Ar3** and more easily separating the final products. As shown in Figure 4, the reaction 3.1 was well controlled at a monoaddition stage by applying an excess amount of **Ar3** to it (**Ar3** to ADIBO-cyclo-RGD = 5:1). RP HPLC analysis indicated that ADIBO-cyclo-RGD was consumed soon after these two starting materials were mixed in water, yielding two products with a ratio of 86% to 14% (Figure 4B, *i*). These two products could readily be separated by HPLC. MALDI mass spectrometry identified that the major product resulted from monoaddition of ADIBO-cyclo-RGD to **Ar3** (**A-2**) and the minor product from the bis-addition. The following reaction was carried in water as well with a 25% excess of **A-2** (Reaction 3.2). As shown in Figure 4B, *ii*, most of ADIBO-anti-thrombin was consumed in a minute. Extending the reaction to 30 min resulted in **RH-2** with a 93% yield and a small amount of bis-addition byproduct (~7%), which was separated by HPLC and characterized with MALDI mass spectrometry (see **RH-2** in Experimetnal Section for details)

In this section, we describe facile methods to synthesize a DNA−organic molecule−DNA (or peptide) conjugate with a high yield and high reaction rate by means of click chemistry. Lee et al. reported a three day reaction of amino functionalized DNA with *N*-hydroxysuccinimide (NHS) ester of 1,3,5-benzenetricarboxylic acid in DMSO/water, which only produced the desired product with a 10% yield.[37] They attribute such a low yield to a consequence of steric hindrance and electrostatic repulsion between DNA molecules. Interestingly, Seela and co-workers reported that a DNA containing a tripropargylamino side chain readily reacted with azido-functionalized oligonucleotides in the presence of a copper catalyst.[38] Since the reaction was accelerated significantly in the presence of benzoic acid, we believe that reduction of the electrostatic repulsion may be a key factor for production of DNA−organic molecule−DNA hybrids with high yields. We have found utilization of Mg^{2+} to shield the negative charges of the DNA backbone could produce the same effects as benzoic acid did (data not shown). Here, we demonstrate that the addition of charged molecules to the three-arm linker can be well controlled simply by changing the solvent.

It should be noted that the ADIBO-azide reaction normally results in a regioisomeric mixture of the triazole connection. In our case, the affinity molecules were connected to **Ar3** through either N-1 or N-3 of the triazole ring (see Figure 2). However, we have not observed that the subtle difference in structure exerts any significant effects on the recognition imaging (vide infra).

Attaching Recognition Heads to AFM Tips. We have previously developed a method to attach affinity molecules through a linear linker to AFM tips using a catalyst-free click reaction.[34] We adopted this method for attachment of these recognition heads. As illustrated in Figure 5, Ni-coated silicon tips (from Nanoworld particularly for recognition imaging) were first functionalized with a cyclooctyne function by reacting with a cyclooctyne derivative of 1-(3′-amino)propylsilatrane (**3**)[34] in aqueous solution, and then reacted with a recognition head in buffered solution (see Experimental Section for details).

DOI: 10.1021/jacs.5b03079
J. Am. Chem. Soc. 2015, 137, 7415−7423

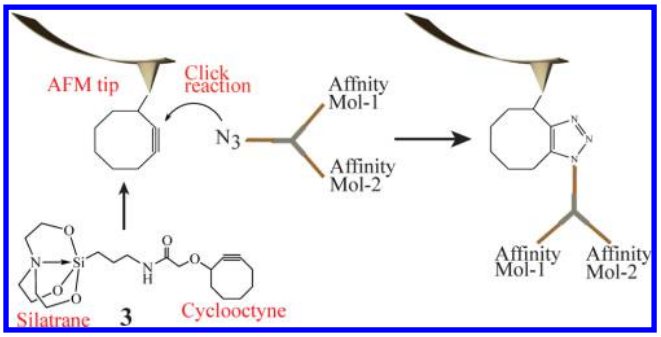

Figure 5. Illustration of attaching a recognition head to an AFM tip using a catalyst free alkyne–azide reaction.

Since there is presently no effective way to characterize the covalent bonding on AFM tips, we attempted to provide evidence that there was a chemical attachment by means of force measurement. We measured the interacting forces of **RH-1** attached to a silicon nitride tip with one of its cognate proteins VEGF. From the force–distance curves, we observe that the binding rupture occurred at a distance around 14 nm, which corresponds to the length of the recognition head plus other carbon chains, and the unbinding force was around 65 pN with a loading rate of 60 nN/s (Figure S2, Supporting Information). This shows the existence of a recognition head on the AFM tip. For the present, we believe that a functional test may be the most direct and best way to prove the successful attachment.

Multiplex Recognition Imaging (mRI) of Proteins. We adapted a procedure reported by Wang et al.[20] to perform mRI experiments, which involves three sequential steps: (1) imaging a protein surface by driving an AFM tip carrying an recognition head across a 2 × 2 μm^2 area and recording the simultaneous topographic and recognition images; (2) injecting a first blocking solution to the liquid flow cell, and repeating the step 1 in the same area; (3) injecting a second blocking solution to the cell and repeating the step 1 again. We first tested **RH-1** on imaging its cognate proteins VEGF and TNFα. A 1:1 mixture of these two proteins in a phosphate buffer (pH 7.4) was deposited on a mica surface functionalized with glutaraldehyde. We have routinely used glutaraldehyde as a cross-linker to immobilize proteins for recognition imaging.[39] Using **RH-1**, we were able to generate recognition images from the VEGF-TNFα surface (Figure S3, Supporting Information). For clarity, a small portion of each full image, taken from the same scanning area, is displayed in Figure 6 for the following discussion. In general, the AFM based recognition imaging produces not only a recognition image, in which the recognition sites appear as dark spots, but also a topographic image simultaneously, in which each feature appears as white.

From the topographic image (Figure 6A), we can immediately notice a complex surface morphology, features of which vary in sizes and shapes. This may reflect differences in structures between VEGF and TNFα as well as effects of the surface chemistry, assuming that each feature represents either an individual protein or a protein aggregate. First, the crystal structures show that VEGF (PDB ID: 2VPF) has approximate dimensions of 6.5 × 3.5 × 2.0 nm, flatter than TNFα (~5.9 × 5.5 × 4.8 nm, PDB ID: 1TNF). Also, both VEGF and TNFα have pI values very close to 7.0 (7.5 for VEGF and 7.4 for TNFα, calculated from http://protcalc.sourceforge.net), so they may easily form aggregates around neutral pH. Second, since glutaraldehyde mainly reacts with lysine residues (11 for VEGF and 5 for TNFα) and the N-terminal amines, the immobilization chemistry may result in each protein molecule displaying on the surface with different orientations. All of these factors may contribute to the complicated surface morphology of the VEGF and TNFα mixture, making it impossible to distinguish between these two proteins from the topography. However, the recognition image (Figure 6B) seems more resolvable. This is because the recognition imaging only "sees" the binding site, a small portion of protein. As an example, the feature in the green circle in Figure 6A could be an aggregate of multiple proteins according to its size ($W \times L \times H$ = ~38 × 80 × 1.6 nm). By examining the recognition image (the green circle in Figure 6B), we can tell that the feature possibly consists of two protein molecules. The following blocking experiments allowed us to unambiguously assign the spot 1 as TNFα and spot 2 as VEGF (to be discussed in the next paragraph). Furthermore, we counted those spots both in Figure 6A,B, and found that there were about 80% features in Figure 6A recognized as protein by **RH-1**. This recognition rate is consistent with our previous results from using AFM tips functionalized with one type of affinity reagent.[34] Since the purity of the protein materials in this study was greater than 95%, we believe that the immobilization chemistry placed a statistical limit on the recognition efficiency because glutaraldehyde randomly reacted with amines of proteins, rendering some of the binding sites blocked by the mica surface and not reachable by the affinity moieties.

Following the first scan, a VEGF solution was injected into the flow cell to block the anti-VEGF aptamer attached to the AFM tip, and the same surface area was scanned again to acquire a second recognition image (Figure 6C). By comparing with Figure 6B, we can clearly see that the spot 1 remained and spot 2 disappeared in Figure 6C. As a result, we could assign these two spots to the corresponding proteins. Presumably, all of the spots in Figure 6C resulted from the anti-TNFα aptamer interacting with the TNFα protein. To confirm this, a TNFα solution was injected into the flow cell, which resulted in an image with no recognition (Figure 6D). The above results

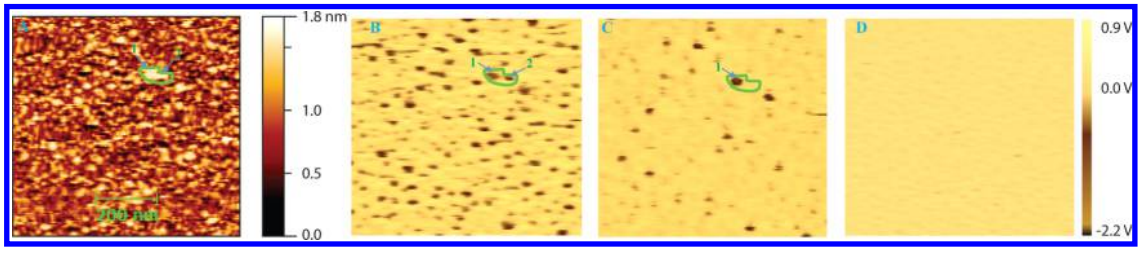

Figure 6. Topographic (A) and recognition (B) image of a VEGF and TNF-α mixture; (C) anti-VEGF aptamer-blocked recognition image; (D) both aptamers-blocked recognition image. Imaging size: 0.75 × 0.75 μm and all of recognition images have the same amplitude scale.

DOI: 10.1021/jacs.5b03079
J. Am. Chem. Soc. 2015, 137, 7415–7423

demonstrate that the two aptamers of **RH-1** can specifically interact with their respective cognate proteins, subject to no interference from each other. To further confirm the specificity of **RH-1**, we scanned a 1:1 mixture of thrombin and streptavidin deposited on the mica surface, which resulted in no recognition image. Therefore, we assign those spots in Figure 6C as the protein TNFα with high confidence. By superimposing the image C on B in Supporting Information Figure S3, we created a superimposed recognition image (Supporting Information Figure S5A), from which we identified all of protein spots in the first recognition image (Supporting Information Figure S3B). Figure 7A shows a portion of the superimposed image in Supporting Information Figure S5A, in which those black topped-by-green spots correspond to the TNFα protein and the rest of black spots to the VEGF protein. By counting the green and black spots in Supporting Information Figure S5A, we determined that the ratio of VEGF to TNFα on the surface is about 0.9:1, close to that in the parent solution (1:1). To further test **RH-1**, we deposited a solution of VEGF and TNF-α mixed in a 5:1 ratio on the mica surface, and found that the recognition efficiency of **RH-1** was still about 80% (determined from image A and B in Figure S4, Supporting Information). In the same fashion as described above, a superimposed image (Supporting Information Figure S5B) was created for identification of individual proteins in Supporting Information Figure S4B. Figure 7B shows a portion of the superimposed image, from which we can clearly see there are less green spots, compared to Figure 7A. The ratio of VEGF to TNFα on the surface was determined as ~5:1 by counting those black and green spots in Supporting Information Figure S5B.

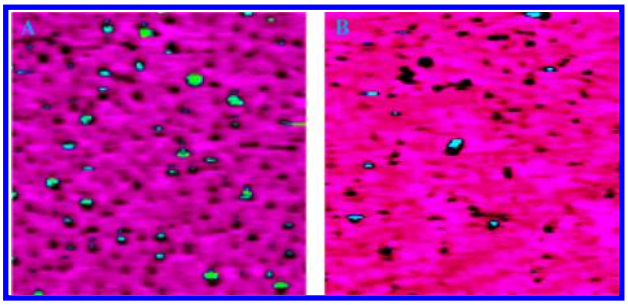

Figure 7. Portion of superimposed recognition images in Supporting Information Figure S5 (enlarged for clarity): (A) acquired from a mixture of VEGF and TNF-α (1:1 in solution) deposited on the mica surface, and (B) from a mixture of VEGF and TNF-α (5:1 in solution) deposited on the mica surface. Black topped-by-green spot, TNF-α protein; black, VEGF protein. Imaging size: 0.75 × 0.75 μm.

We further tested **RH-1** on a more complex mixture consisting of four proteins VEGF, TNF-α, thrombin, and streptavidin. First, we examined the specificity of mRI by performing a series of control experiments: using a **RH-1** tip to scan a mica surface modified with a 1:1 mixture of thrombin and streptavidin, which only yielded a topographic image (Figure 8A), but no recognition image (Figure 8A′); using a bare AFM tip and a tip functionalized with the cyclooctyne **3** to scan a surface modified with a VEGF and TNFα mixture, which again only yielded topographic images (Figure 8B and 8C), and no recognition images (Figure 8B′ and 8C′). When scanning a mica surface on which a mixed solution of four proteins (VEGF/TNFα/thrombin/streptavidin = 1:1:2:1.5) was deposited, we were able to obtain both topographic and recognition images (Figure 8D,D′) using a tip functionalized with **RH-1**. There were 26% of proteins in Figure 8D recognized, a 72% recognition rate which is slightly smaller than what we have had from the mixture of two proteins. The recognition specificity was confirmed by blocking experiments (Figure S6 in Supporting Information). In the same manner as described above, the ratio of VEGF/TNFα on the surface was determined as 1.5:1, higher than that in their parent solution. Nonetheless, this is the first demonstration that the recognition imaging is able to detect multiple proteins in such a complex mixture.

Next, we tested **RH-2** for mRI with a 1:1 mixed solution of thrombin and integrin $\alpha_5\beta_1$ deposited on the mica surface. Similarly, **RH-2** yielded a recognition image with 80% of protein in the topographic image recognized (Figure 9A,B). From the superimposed recogntion image (Figure 9E) generated by overlapping the image C over B in Figure 9, we determined the ratio of thrombin to integrin $\alpha_5\beta_1$ on the surface as 1:0.9. Note that those pale yellow spots in the recognition image C and D in Figure 9 may be caused by the

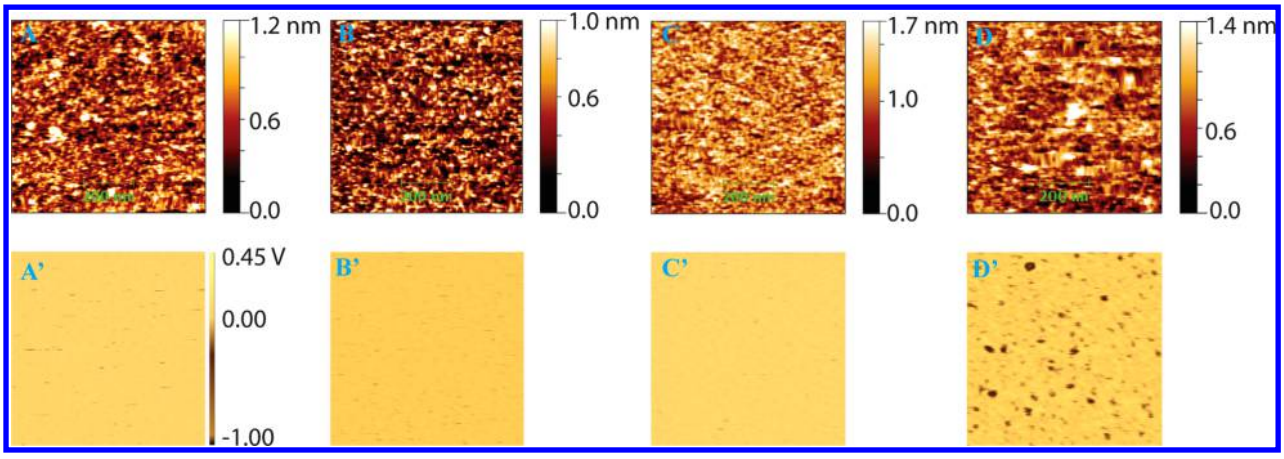

Figure 8. AFM images with different tips and substrates. Top panel: topographic image of (A) a tip functionalized with **RH-1** against a 1:1 mixture of thrombin and streptavidin deposited on mica; (B) a bare tip against a 1:1 mixture of VEGF and TNF-α deposited on mica, (C) a tip functionalized with cyclooctyne against a 1:1 mixture of VEGF and TNF-α deposited on mica, (D) a tip functionalized with **RH-1** against a mixture of VEGF, TNF-α, thrombin and streptavidin deposited on mica. Bottom panel: recognition image of A′ relating to topographic image A, B′ to B, C′ to C, and D′ to D. All of recognition images have the same amplitude scale. Imaging size: 0.75 × 0.75 μm.

DOI: 10.1021/jacs.5b03079
J. Am. Chem. Soc. 2015, 137, 7415−7423

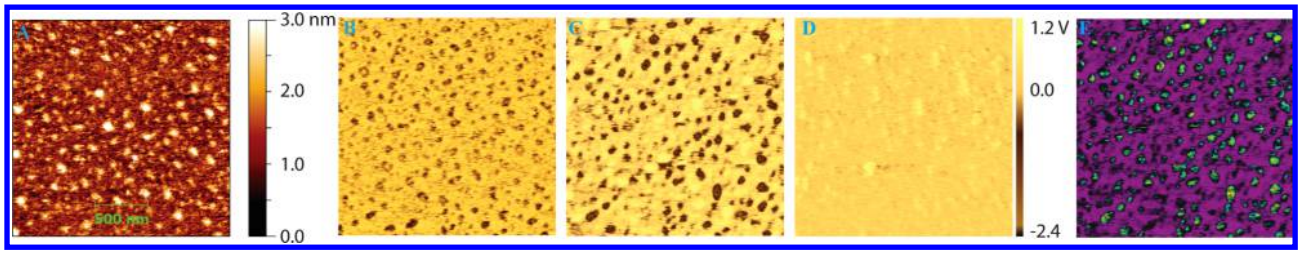

Figure 9. Topographic (A) and recognition (B) image of a thrombin and integrin $\alpha_5\beta_1$ mixture; (C) recognition image from blocking anti-thrombin aptamer; (D) recognition image from blocking both aptamer and RGD; (E) superimposed recognition image of C over B. Black topped-by-green spot, integrin; black, thrombin. Imaging size: 2 × 2 μm and all of recognition images have the same amplitude scale.

spillover of amplitude from topographic image to recognition image.[40] We also notice that the measured ratios in all the cases varied from those in the sample solutions more or less. To fully understand the discrepancies, thus, further studies are needed on molecular immobilization and on thermodynamic and kinetic effects on interactions of the affinity molecule tethered to an AFM tip with its cognate protein immobilized on the surface.

SUMMARY

In the present study, we have developed a new approach to using AFM for multiplex recognition imaging. With a recognition head attached to an AFM tip, we were able to scan multiple proteins immobilized on a surface. The recognition head was designed based on a hypothesis that two affinity molecules connected by a well-spaced linker should interact with their respective cognate molecules effectively. Our studies have shown that the affinity molecules tethered to the three-arm linker worked independently and equally, which allowed us not only to identify two different proteins but also to relatively quantitate them by counting. In our current setup, it only needs 2 to 3 μL of protein solution with a concentration of ~2 ng/mL for each imaging experiment. We end by considering some possible applications of this new technique. Since multiplexing has become increasingly important for molecular diagnostics of diseases in clinics,[41] one example would be measurement of the ratios of free prostate-specific antigen (fPSA) and complexed prostate-specific antigen (cPSA) using a recognition head composed of anti-fPSA and cPSA antibodies for distinguishing between benign prostatic hyperplasia (BPH) and prostate cancer when the total PSA is in a "gray zone" range of 4−10 ng/mL.[42] If free PSA is less than 25%, a patient's high total PSA may suggest cancer. In contrast to conventional immunoassays,[43] mRI provides a means to simultaneously measure fPSA and cPSA in a sample at a single molecule level. As a second example, given its single molecule detection and nanometer resolution, the AFM-based mRI should be useful in analysis of proteins in multisubunit complexes, such as nucleosomes. A nucleosome is composed of eight histones, typically two histone (H2A/H2B) dimers and a histone $(H3/H4)_2$ tetramer, wrapped with DNA. We can conceive of using the mRI to detect the H2A/H2B dimer and its H2A.Z/H2B variant in nucleosomes.[44]

With a perspective on applying mRI to biological research and clinical diagnostics, we are aware of the importance of accessibility of the method. We believe that our synthetic method, which has features of one-step synthesis of the three-arm linker and highly yielded conjugating reactions, should be easy to scale up for manufacture. For proof of the recognition head concept, we have taken advantages of nucleic acid and peptide aptamers, which have smaller sizes compared to antibodies, and are rapidly available by custom-synthesis as well as can be modified at will. Currently, we are developing an effective method for a recognition head carrying antibody pairs to broaden applications of the mRI technique.

EXPERIMENTAL SECTION

General Information. All reagents and solvents were purchased from commercial suppliers (Sigma-Aldrich, Alfa Aesar, Fluka, TCI America) and used as received unless otherwise noted. All experiments requiring anhydrous conditions were performed in flame-dried glassware under nitrogen atmosphere. Reactions were monitored by thin layer chromatography (TLC) using silica gel precoated on glass plates (EMD Millipore). ^{1}H NMR and ^{13}C NMR spectra were recorded on Varian INOVA 400 (400 MHz) spectrometer at 25 °C. Chemical shifts (δ) are given in parts per million (ppm) and referenced to the residual solvent peak ($CDCl_3$, δ_H = 7.26 ppm; CD_3OD, δ_H = 3.31 ppm; DMSO-d_6, δ_H = 2.50 ppm). Coupling constants (J) are expressed in hertz (Hz) and the values are rounded to the nearest 0.1 Hz. Splitting patterns are reported as follows: br, broad; s, singlet; d, doublet; dd, doublet of doublets; t, triplet; dt, doublet of triplets; q, quartet and m, multiplet. High-resolution mass spectra (HRMS) were acquired at the Arizona State University CLAS High Resolution Mass Spectrometry Facility. Flash chromatography was performed in an automated flash chromatography system (CombiFlash R_f, Teledyne Isco, Inc.) with silica gel columns (60−120 mesh). RP-HPLC analysis and separation were performed with either a Zorbax C-18 column or with Zorbax 300 SB-C18 column (4.6 × 150 mm, particle size 5 μm) in an Agilent 1100 HPLC equipped with UV monitor and fraction collector.

VEGF (Vascular Endothelial Growth Factor, Human Recombinant, 95%), a lyophilized product from a concentrated (1 mg/mL) solution with no additives, TNFα (Tumor Necrosis Factor-Alpha, Human Recombinant, 95%), a lyophilized product from 1 mg of TNF-α Human contain 20 mM PB, pH-7.2, and 100 mM NaCl were purchased from ProSpec; Integrin from Yo proteins AB (Sweden), a lyophilized product from a solution containing 0.26 mg/mL $\alpha_5\beta_1$, 20 mM Tris-HCl pH 7.5, 150 mM NaCl, 2 mM $MgCl_2$, 0.2% Triton X-100. They were reconstituted by dissolving in water before use according to manufacture recommendation. Human α-thrombin and streptavidin were purchased from AbCam and Alfa Aesar, respectively.

Recognition imaging was performed on Agilent's MacMode AFM equipped with a PicoTREC system, and silicon tips purchased from NanoWorld. The cantilever was made having length of 125 μm, width of 35 μm, and thickness of 800 nm with a force constant of 0.14 N/m. Its backside was coated with 1 nm Ti/40 nm Ni.

*1,3,5-Tris{[4-(1-azido-3n$_{36}$^{3}-dodecoxaheptatriacontyl)phenyl]-ethynyl}benzene (**Ar3**).* 1,3,5-Triethynylbenzene (**1**, 62 mg, 0.41 mmol) and compound **2** (1.0 g, 1.27 mmol) were mixed in anhydrous tetrahydrofuran (7.5 mL) and triethylamine (7.5 mL) under nitrogen. The solution was degassed by slowly bubbling nitrogen for 10 min, to which bis(triphenylphosphine)palladium(II)dichloride (14.4 mg, 0.02 mmol) and copper(I) iodide (3.9 mg, 0.02 mmol) were added. The mixture was refluxed for 48 h, cooled to room temperature, and filtered. The solvent was removed by rotary evaporation. The residue

DOI: 10.1021/jacs.5b03079
J. Am. Chem. Soc. 2015, 137, 7415−7423

was separated by silica gel column chromatography with a gradient of 4% methanol in dichloromethane over 4 h. The product **Ar3** was obtained as a yellowish oil (307 mg, 35%). ^{1}H NMR (400 MHz, $CDCl_3$): δ 3.36 (t, J = 5.2 Hz, 6H, N_3CH_2); 3.62−3.68 (m, 138H, OCH_2CH_2O); 4.58 (s, 6H, $ArCH_2$); 7.33 (d, J = 8.4 Hz, 6H, ArH); 7.49 (d, J = 8.4 Hz, 6H, ArH); 7.62 (s, 3H, Ar'H). ^{13}C NMR (100 MHz, $CDCl_3$): δ = 139.03, 133.97, 131.68, 127.58, 124.02, 121.90, 90.43, 87.75, 72.79, 70.68−70.56, 70.01, 69.66, 50.67. MALDI-MS (M + Na): found m/z 2152.51; calcd for $C_{105}H_{165}N_9O_{36}Na$ 2152.46.

RH-1. A solution of **Ar3** in water (400 μM, 30 μL) was added to a solution of ADIBO-anti-VEGF in water (200 μM, 30 μL). After 1 min, the reaction was checked by injecting 1 μL of the reaction solution into RP-HPLC. The HPLC analysis indicated that the aptamer was fully consumed and a new peak appeared at a retention time of 18.0 min in the chromatogram (eluent A, 10 mM TEAA buffer, pH 7; eluent B, acetonitrile; under a linear gradient of increasing B from 10 to 70% in 25 min). The monoaddition product **A-1** was separated using HPLC with the same eluting system. MALDI-MS (M + H): found m/z 10401.8; calcd for $C_{381}H_{513+1}N_{110}O_{187}P_{25}$ 10402.2. Next, **A-1** (150 μM, 15 μL) was mixed with ADIBO-anti-TNFα (75 μM, 15 μL) in a TEAA buffer (50 mM, pH 7). The reaction was kept at room temperature for 1 h and separated using the same HPLC conditions for the monoaddition product. **RH-1** has retention time of 14.5 min. MALDI-MS (M + H): found m/z 18768.6; calcd for $C_{659}H_{861+1}N_{215}O_{339}P_{50}$ 18766.7.

RH-2. A solution of **Ar3** in water (1.0 mM, 30 μL) was added to a solution of ADIBO-cycloRGD in water (0.2 mM, 30 μL). The solution was checked by HPLC after 1 min. RP-HPLC analysis indicated that the peptide was completely consumed and a new peak appeared at retention time of 25.1 min in the chromatogram under the same elution conditions as the one for **RH-1**. The monoaddition product **A-2** was separated by HPLC. MALDI-MS (M + H): found m/z 3050.2; calcd for $C_{153}H_{223+1}N_{19}O_{45}$ 3049.5. **A-2** (100 μM, 15 μL) was mixed with ADIBO-anti-thrombin (80 μM, 15 μL) in water. The reaction was stirred at room temperature for 30 min. **RH-2** was separated by RP HPLC under the same conditions mentioned above. The product has retention time of 15.1 min. MALDI-MS (M + H): found m/z 8349.2; calcd for $C_{336}H_{453+1}N_{78}O_{144}P_{15}$ 8354.2.

Attaching Recognition Heads to AFM Tips. AFM tips (a batch of four) were first soaked in ethanol in a Petri dish for 5 min, dried with nitrogen, and then treated with oxygen plasma (medium power) for 2 min in a Harrick Plasma Cleaner and then with ultraviolet-ozone in a Boekel UV cleaner for 5 min. These tips were immersed in an aqueous solution of *N*-(3-(silatranyl)propyl)-2-(cyclooct-2-yn-1-yloxy)acetamide (**3**, 50 mM) in a Petri dish. After 1 h, the tips were taken out, rinsed with water thrice, and dried gently with a nitrogen flow. In a humid surrounding, the cyclooctyne-functionalized tips were placed in a Petri dish and a recognition head solution (10 μM, 20 μL) in 1× PBS buffer (pH 7.4) was added to cover all the tips. After 1 h, the tips were rinsed thrice with the same buffer and used immediately for AFM measurements. However, the probes can be stored in 1× PBS buffer (pH 7.4) at 4 °C at least for 2 days. Normally, there were about 50% of them that worked effectively for recognition experiments in every batch of 4 to 5 functionalized tips

Protein Immobilization. First, a mica surface was functionalized following an APTES/glutaraldehyde procedure developed in our laboratory.[39] Then, a protein solution (3 μL) was added to the glutaraldehyde-coated mica in a humid chamber, incubated for 30 min, rinsed with a 1× PBS buffer (pH 7.4) three times, and immediately placed on the AFM stage for use. The following solutions were used for the study:

A mixed solution of VEGF and TNF-α (0.35 nM each)

A mixed solution of VEGF (0.48 nM) and TNF-α (0.1 nM)

A mixed solution of VEGF (0.1 nM), TNF-α (0.1 nM), thrombin (0.2 nM) and streptavidin (0.15 nM)

A mixed solution of thrombin (0.28 nM) and streptavidin (0.28 nM)

A mixed solution of integrin $\alpha_5\beta_1$ and thrombin (0.3 nM each).

Multiplex Recognition Imaging. AFM images were acquired by PicoTrec using magnetically (Ni) coated cantilevers in AC (MAC) mode operation with AC frequency at 8 kHz, set point of 4 V, and a scan speed of 2.2 μm/s. For imaging with **RH-1** functionalized tips, the protein deposited on the mica surface was covered with 1× PBS buffer (pH 7.4, 600 μL). After initial scanning, a first blocking solution (0.3 nM VEGF in 1× PBS buffer, pH 7.4, 50 μL) was injected to the flow cell, incubated for 10 min, and followed by scanning in the same area. A second blocking solution (0.6 nM TNF-α in 1× PBS buffer, pH 7.4, 50 μL) was injected into the flow cell, incubated for 10 min, followed by scanning in the same area. Four samples were examined with **RH-1**: two mixed solutions of VEGF and TNFα, respectively, with 1:1 and 5:1 molar ratios, a mixed solution consisting of VEGF, TNF, thrombin, and streptavidin with a ratio of 1:1:2:1.5, and a mixed solution of thrombin and streptavidin with a 1:1 molar ratio.

For imaging with **RH-2** functionalized tips, a mixed solution of thrombin and integrin $\alpha_5\beta_1$ with a 1:1 molar ratio was deposited on the mica surface and covered with 1× PBS buffer containing 1 mM $MnCl_2$ (pH 7.4, 600 μL). The experiment was carried out in the same way as described above, and two blocking solutions, integrin (0.2 nM in 1× PBS buffer, pH 7.4, 50 μL) and thrombin (0.15 nM in 1× PBS buffer, pH 7.4, 50 μL), were used sequentially.

Note: in some cases, injection of additional blocking solution (50 μL) was needed in order to achieve the effective blocking.

Data Analysis. All of the topographic and recognition images, and force spectra were recorded using Agilent PicoView software. Topography images presented in the manuscript were processed in Gwyddion software. Those spots were counted as proteins with a threshold around 1 nm.

The recognition images were analyzed using Picoview. Background noises of the recognition images were scaled about −50 mV. Typical recognition events were observed to have intensity between −100 mV and −1.2 V. To determine the recognition rates, topography and recognition images were saved as image files and superimposed in Adobe Photoshop. The numbers of unrecognized and recognized proteins were manually counted from the superimposed image. In the same fashion, individual proteins were identified by image superimposing and manually counting.

■ ASSOCIATED CONTENT

Supporting Information

Detailed descriptions of synthesis and characterization of compound **2**, ADIBO derivatives of affinity molecules, and additional recognition images. The Supporting Information is available free of charge on the ACS Publications website at DOI: 10.1021/jacs.5b03079.

■ AUTHOR INFORMATION

Corresponding Authors

*Stuart.Lindsay@asu.edu

*Peiming.Zhang@asu.edu

Notes

The authors declare the following competing financial interest(s): The authors declare the following competing financial interest(s): P.Z., S.L., S.M., and S.S. are named as inventors on related patent applications.

■ ACKNOWLEDGMENTS

This research was supported by a Grant (U54CA143862) from National Cancer Institute (NCI). We would like to thank Natalya Zolotova for HRMS measurements, and Dr. Weisi Song for his help in drawing Figure 1.

■ REFERENCES

(1) Muller, D. J.; Dufrene, Y. F. *Nat. Nanotechnol.* **2008**, *3*, 26.
(2) Engel, A.; Müller, D. J. *Nat. Struct. Biol.* **2000**, *7*, 715.

DOI: 10.1021/jacs.5b03079
J. Am. Chem. Soc. 2015, 137, 7415−7423

(3) Alsteens, D.; Dupres, V.; Yunus, S.; Latge, J. P.; Heinisch, J. J.; Dufrene, Y. F. *Langmuir* **2012**, *28*, 16738.
(4) Rudnev, A. V.; Malinovskii, V. L.; Nussbaumer, A. L.; Mishchenko, A.; Häner, R.; Wandlowski, T. *Macromolecules* **2012**, *45*, 5986.
(5) Zhang, J.; Chen, P.; Yuan, B.; Ji, W.; Cheng, Z.; Qiu, X. *Science* **2013**, *342*, 611.
(6) Embrechts, A.; Schonherr, H.; Vancso, G. J. *J. Phys. Chem. B* **2008**, *112*, 7359.
(7) Lin, S.; Chen, J.-L.; Huang, L.-S.; Lin, H.-W. *Curr. Proteomics* **2005**, *2*, 55.
(8) Sikora, A. E.; Smith, J. R.; Campbell, S. A.; Firman, K. *Soft Matter* **2012**, *8*, 6358.
(9) Sorci, M.; Dassa, B.; Liu, H.; Anand, G.; Dutta, A. K.; Pietrokovski, S.; Belfort, M.; Belfort, G. *Anal. Chem.* **2013**, *85*, 6080.
(10) Ritzefeld, M.; Walhorn, V.; Anselmetti, D.; Sewald, N. *Amino Acids* **2013**, *44*, 1457.
(11) Florin, E.-L.; Moy, V. T.; Gaub, H. E. *Science* **1994**, *264*, 415.
(12) Thormann, E.; Simonsen, A. C.; Nielsen, L. K.; Mouritsen, O. G. *J. Mol. Recognit.* **2007**, *20*, 554.
(13) Lee, C. K.; Wang, Y. M.; Huang, L. S.; Lin, S. *Micron* **2007**, *38*, 446.
(14) Ando, T.; Uchihashi, T.; Kodera, N. *Annu. Rev. Biophys.* **2013**, *42*, 393.
(15) Preiner, J.; Kodera, N.; Tang, J.; Ebner, A.; Brameshuber, M.; Blaas, D.; Gelbmann, N.; Gruber, H. J.; Ando, T.; Hinterdorfer, P. *Nat. Commun.* **2014**, *5*, 4394.
(16) Dufrene, Y. F. *Proteomics* **2009**, *9*, 5400.
(17) Lekka, M. *Nat. Nanotechnol.* **2012**, *7*, 691.
(18) Stroh, C.; Wang, H.; Bash, R.; Ashcroft, B.; Nelson, J.; Gruber, H.; Lohr, D.; Lindsay, S. M.; Hinterdorfer, P. *Proc. Natl. Acad. Sci. U.S.A.* **2004**, *101*, 12503.
(19) Zhu, R.; Howorka, S.; Proll, J.; Kienberger, F.; Preiner, J.; Hesse, J.; Ebner, A.; Pastushenko, V. P.; Gruber, H. J.; Hinterdorfer, P. *Nat. Nanotechnol.* **2010**, *5*, 788.
(20) Wang, H.; Bash, R.; Lohr, D. *Anal. Biochem.* **2007**, *361*, 273.
(21) Beal, D. M.; Jones, L. H. *Angew. Chem., Int. Ed.* **2012**, *51*, 6320.
(22) Viault, G.; Dautrey, S.; Maindron, N.; Hardouin, J.; Renard, P. Y.; Romieu, A. *Org. Biomol. Chem.* **2013**, *11*, 2693.
(23) Chinchilla, R.; Najera, C. *Chem. Rev.* **2007**, *107*, 874.
(24) Lin, L.; Wang, H.; Liu, Y.; Yan, H.; Lindsay, S. *Biophys. J.* **2006**, *90*, 4236.
(25) Kienberger, F.; Ebner, A.; Gruber, H. J.; Hinterdorfer, P. *Acc. Chem. Res.* **2006**, *39*, 29.
(26) Martinez-Veracoechea, F. J.; Leunissen, M. E. *Soft Matter* **2013**, *9*, 3213.
(27) Potty, A. S.; Kourentzi, K.; Fang, H.; Jackson, G. W.; Zhang, X.; Legge, G. B.; Willson, R. C. *Biopolymers* **2009**, *91*, 145.
(28) Orava, E. W.; Jarvik, N.; Shek, Y. L.; Sidhu, S. S.; Gariepy, J. *ACS Chem. Biol.* **2013**, *8*, 170.
(29) Bock, L. C.; Griffin, L. C.; Latham, J. A.; Vermaas, E. H.; Toole, J. J. *Nature* **1992**, *355*, 564.
(30) Macaya, R. F.; Schultze, P.; Smith, F. W.; Roet, J. A.; Feigon, J. *Proc. Natl. Acad. Sci. U.S.A.* **1993**, *90*, 3745.
(31) Haubner, R.; Gratias, R.; Diefenbach, B.; Goodman, S. L.; Jonczyk, A.; Kessler, H. *J. Am. Chem. Soc.* **1996**, *118*, 7461.
(32) Berezovski, M.; Nutiu, R.; Li, Y.; Krylov, S. N. *Anal. Chem.* **2003**, *75*, 1382.
(33) Bochen, A.; Marelli, U. K.; Otto, E.; Pallarola, D.; Mas-Moruno, C.; Leva, F. S. D.; Boehm, H.; Spatz, J. P.; Novellino, E.; Kessler, H.; Marinelli, L. *J. Med. Chem.* **2013**, *56*, 1509.
(34) Senapati, S.; Manna, S.; Lindsay, S.; Zhang, P. *Langmuir* **2013**, *29*, 14622.
(35) Debets, M. F.; van Berkel, S. S.; Schoffelen, S.; Rutjes, F. P.; van Hest, J. C.; van Delft, F. L. *Chem. Commun.* **2010**, *46*, 97.
(36) Kuzmin, A.; Poloukhtine, A.; Wolfert, M. A.; Popik, V. V. *Bioconjugate Chem.* **2010**, *21*, 2076.
(37) Lee, J. K.; Jung, Y. H.; Tok, J. B.-H.; Bao, Z. *ACS Nano* **2011**, *5*, 2067.
(38) Xiong, H.; Leonard, P.; Seela, F. *Bioconjugate Chem.* **2012**, *23*, 856.
(39) Wang, H.; Bash, R.; Yodh, J. G.; Hager, G. L.; Lohr, D.; Lindsay, S. M. *Biophys. J.* **2002**, *83*, 3619.
(40) Wildling, L.; Unterauer, B.; Zhu, R.; Rupprecht, A.; Haselgrubler, T.; Rankl, C.; Ebner, A.; Vater, D.; Pollheimer, P.; Pohl, E. E.; Hinterdorfer, P.; Gruber, H. J. *Bioconjugate Chem.* **2011**, *22*, 1239.
(41) Gokmen-Polar, Y.; Badve, S. *Sci. Transl. Med.* **2014**, *6*, 219fs3.
(42) Prensner, J. R.; Rubin, M. A.; Wei, J. T.; Chinnaiyan, A. M. *Sci. Transl. Med.* **2012**, *4*, 127rv3.
(43) Kort, S. A.; Martens, F.; Vanpoucke, H.; van Duijnhoven, H. L.; Blankenstein, M. A. *Clin. Chem.* **2006**, *52*, 1568.
(44) Luk, E.; Ranjan, A.; Fitzgerald, P. C.; Mizuguchi, G.; Huang, Y.; Wei, D.; Wu, C. *Cell* **2010**, *143*, 725.

DOI: 10.1021/jacs.5b03079
J. Am. Chem. Soc. 2015, 137, 7415−7423